Electronic Supplementary Material (ESI) for Analytical Methods.

Supplementary Information

Fluorescent microRNA Biosensors: A comparison of signal generation to quenching

C. Kyle Almlie, Nicholas E. Larkey, and Sean M. Burrows*

153 Gilbert Hall, Corvallis, OR 97331, United States of America

Email: sean.burrows@oregonstate.edu

Comparison of baseline fluorescent signals of the RQ hairpin

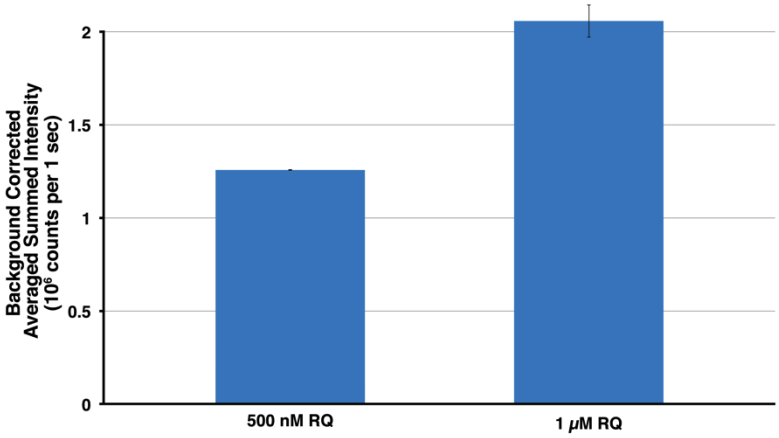

Figure S1. Demonstration of the difference in fluorescence intensity from the hairpin configuration of 500 nM and 1 μM RQ. Signal arises from incomplete quenching by Iowa Black Red Quencher and equilibrium between open and closed hairpin states during signal acquisition. From thermodynamic predictions about 1.3 and 2.6 nM of RQ are open for the 500 nM and 1 μM RQ solutions, respectively. Having fewer fluorescent dyes in solution allows for a lower background, which correlates to a higher sensitivity. (N = 3)

Homodimer considerations

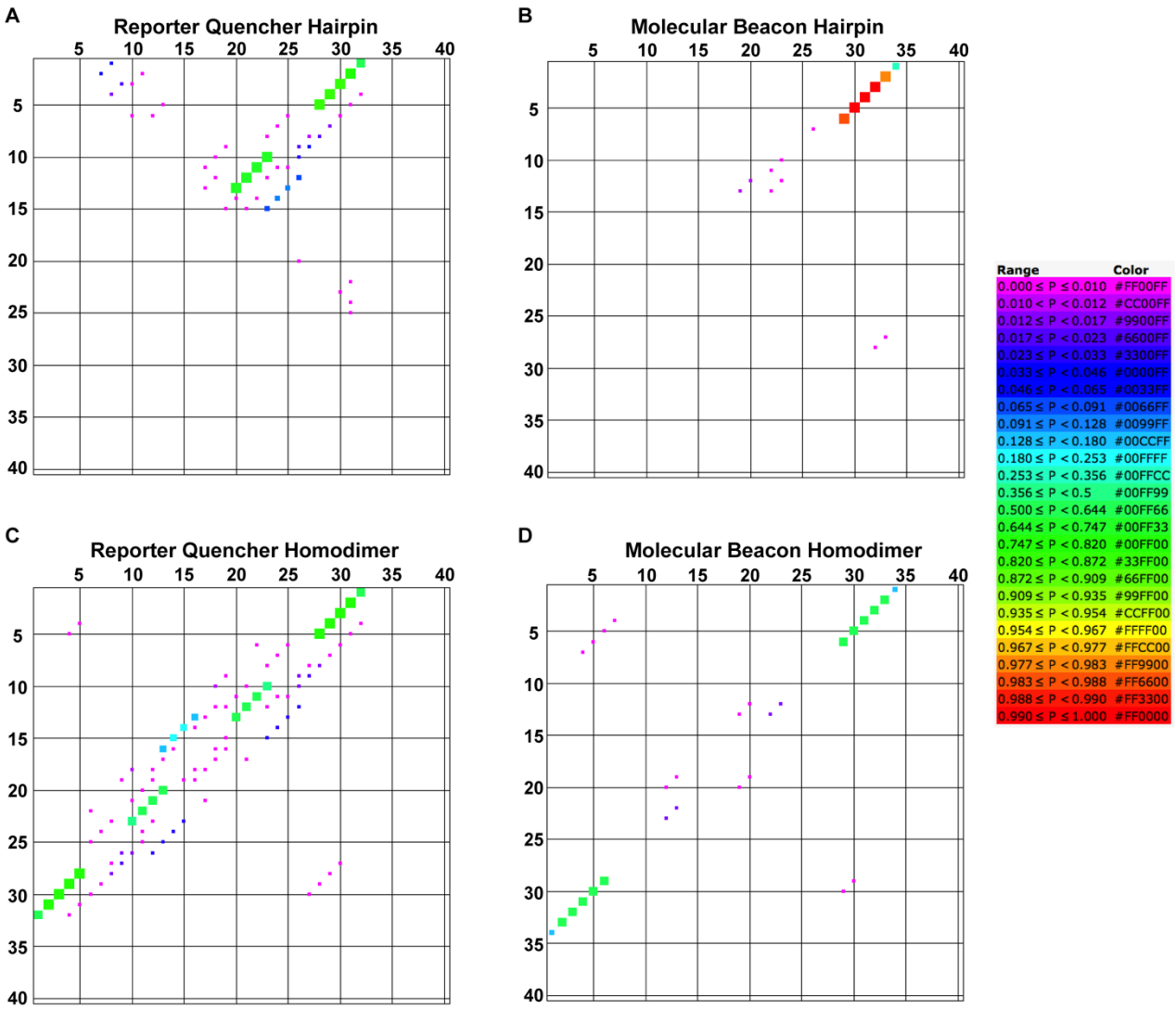

Figure S2. Comparison of probabilities[27-29] for (A) RQ and (B) MB hairpins as well as homodimers for (C) RQ and (D) MB (color and size of boxes represent probability, axis numbering starts from 5 prime end of strand). The stem binding of MB hairpin is greater than RQ (compare A and B). The probability of MB stem base pairing is greater than the MB homodimer base pairing (compare B and D). For the RQ, there is equal probability for base pairing in either the homodimer or the hairpin (compare A to C). From a probability stand point the RQ will probably have more

homodimers than MB. The probability analysis coupled with greater thermodynamic stability of homodimers for both MB and RQ supports the argument that an equilibrium may exist between hairpins and homodimers. However, the very small instrumental error does not support the claim that the equilibrium will influence all of the fluorescence results.

Base pairs in the (RQ+P) biosensor

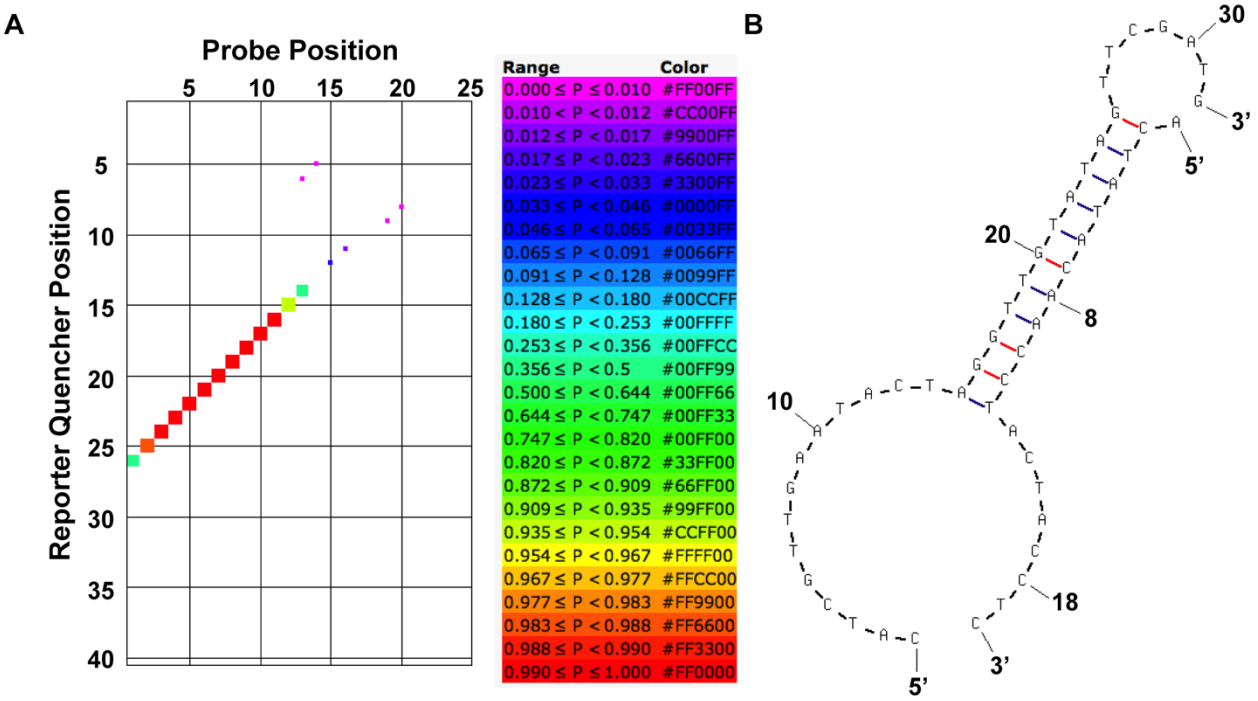

Figure S3. (A) shows the probability[27-29] of base pair formation for the (RQ+P) biosensor (1 μM RQ and 500 nM P; color and size of boxes represent probability, axis numbering starts from 5 prime end of strand). Half the time there are 11 base pairs and the other half the time there are 13 base pairs. The dynamic nature of the (RQ+P) biosensor most likely aids in the displacement reaction upon miRNA addition. (B) Corresponding structure prediction using Energy Minimization Rules.[27-29]

Relationship between predicted K_A values, equilibrium concentrations, and signal intensity for RQ and MB hairpins

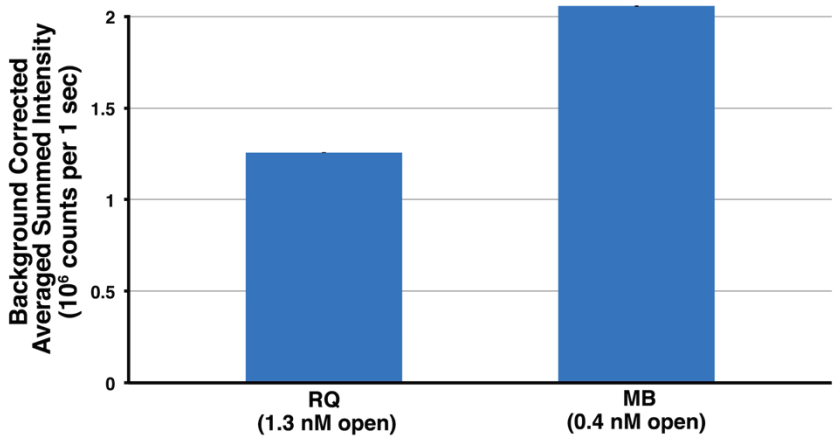

Figure S4. Comparison between the fluorescent signals (N = 3) of the RQ and MB hairpins (500 nM). Even in the hairpin configuration, an equilibrium exists between open and closed hairpin configurations, with a small proportion of either reporter molecule being open. The predicted K_A values of the hairpin configuration for RQ and MB give equilibrium concentrations of 1.3 nM RQ open and 0.4 nM MB open. However, RQ demonstrates more quenching than MB even though the amount of open RQ is greater than MB. One reason for this observation is that the Cy5 on RQ is closer to a terminal Guanine, a known quencher, than the Cy5 on the MB. The other reason is due to the prediction that the terminal A-T base pair on the end of the MB stem is only formed 50 % of the time. This suggests the Cy5-quencher distance is dynamic and averaged to a higher value.

Secondary structure considerations of (MB+let-7a), (RQ+P), and (RQ+RT)

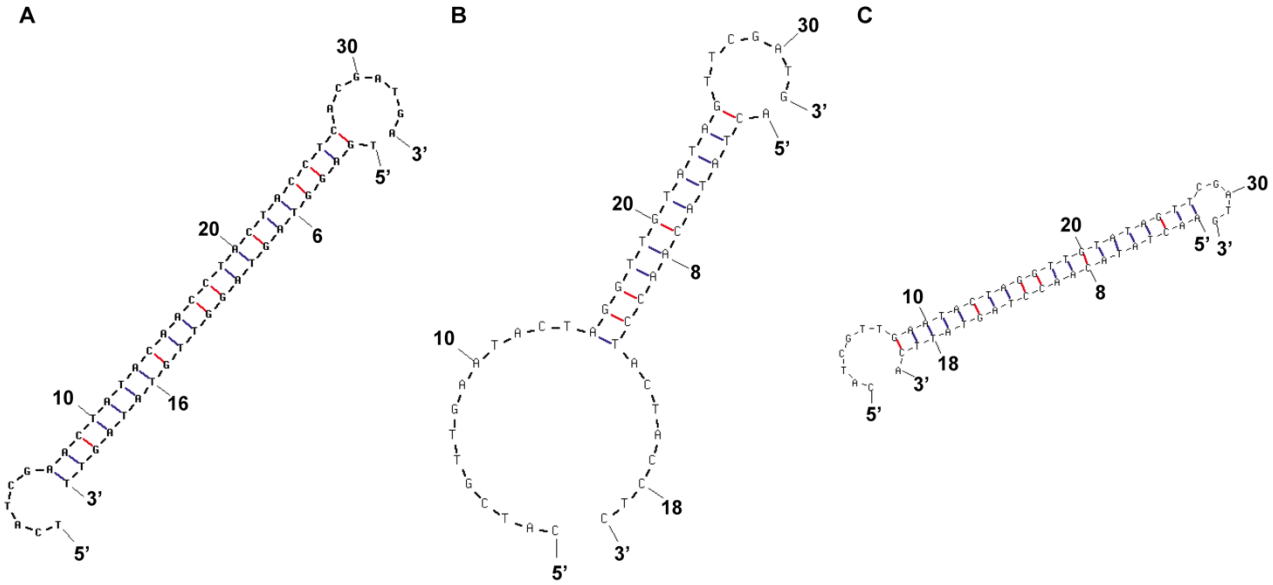

Figure S5. Differences in signal among different heterodimers are related to comparison of secondary structure[27-29] for (A) (MB+let-7a), (B) (RQ+P), and (C) (RQ+RT). The (MB+Let7a) is simply longer than RQ and has a terminal Adenine and Thymine that contribute less to quenching. In contrast, RQ has a terminal Guanine and Cytosine that exhibit more quenching. The (RQ+P) also has a long non-complementary region that could permit the 5' Cy5 on the reporter to interact with nucleic acids on 3' end of the probe in such a way that quenching occurs. Finally in (RQ+RT) there are fewer unpaired nucleic acids and thus fewer chances of interactions like (RQ+P). Furthermore the increased complementarity of the RT forces Cy5 and quencher farther apart. Predictions were made with 1 μM MB and 500 nM Let-7a, 1 μM RQ and 500 nM P, and 1 μM RQ and 500 nM RT.

Signal, Noise, and Cuvette Error analysis of various reporter configurations

A. RQ Hairpin – zoomed in 6 replicates

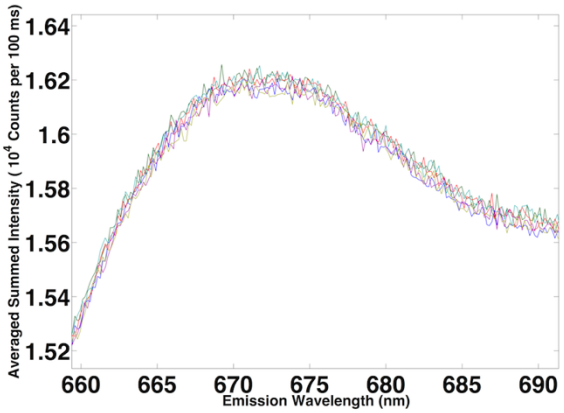

B. RQ Hairpin – zoomed in 18 replicates (6 frames and 3 cuvette placements)

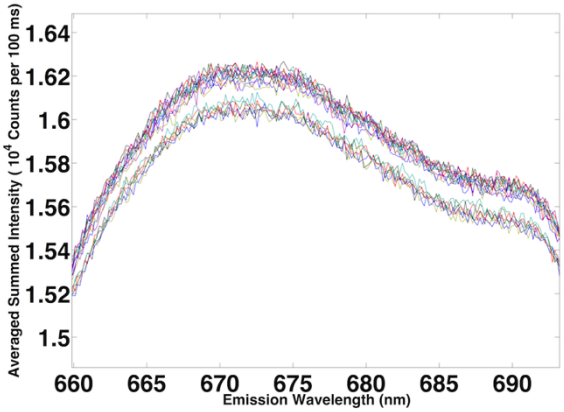

C. RQ Hairpin – zoomed out 18 replicates (6 frames and 3 cuvette placements)

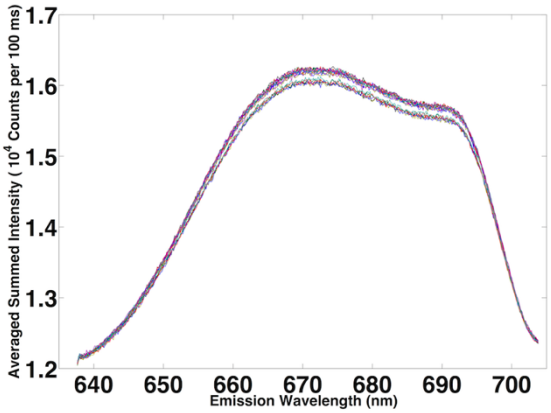

D. (RQ+P) complex – zoomed in 6 replicates

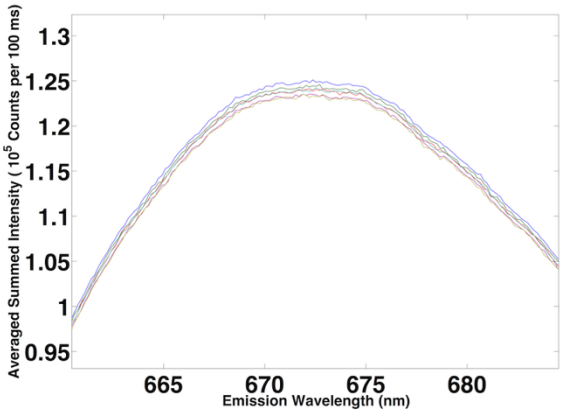

E. (RQ+P) – zoomed in 18 replicates (6 frames and 3 cuvette placements)

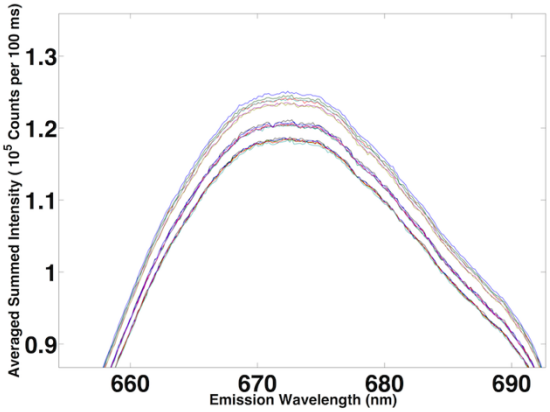

F. (RQ+P) – zoomed out 18 replicates (6 frames and 3 cuvette placements)

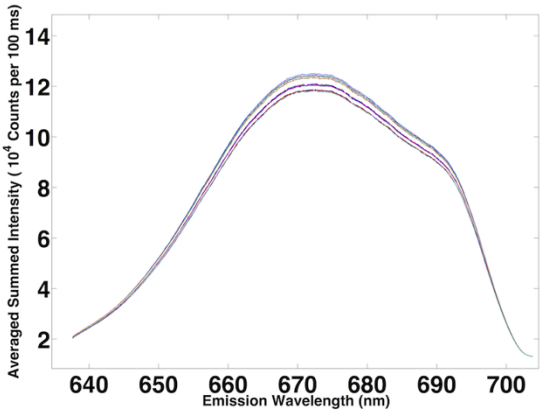

Figure S6. The figures above show the origins of the signal-to-noise ratios and how the large error bars in Figure 6 arise. S3A, S3D show good signal-to-noise for 6 frames (1 cuvette placement) with the RQ in the hairpin and probe-bound configurations, respectively. S3B, S3E are zoomed-in on the peaks to show the variation of signal intensity and the origin of the large error bars from the 3 cuvette placements (18 frames). This figure shows the large variation in S/N is not representative of the signal-to-noise ratio of a single cuvette placement. S3C, S3F are the zoomed-out versions of S3B, S3E to show overall variation of signal due to the three cuvette placements. All solutions are 500 nM RQ. Note: The sharp cutoff beginning at 695 nm is due to a 705 nm long-pass dichroic mirror.

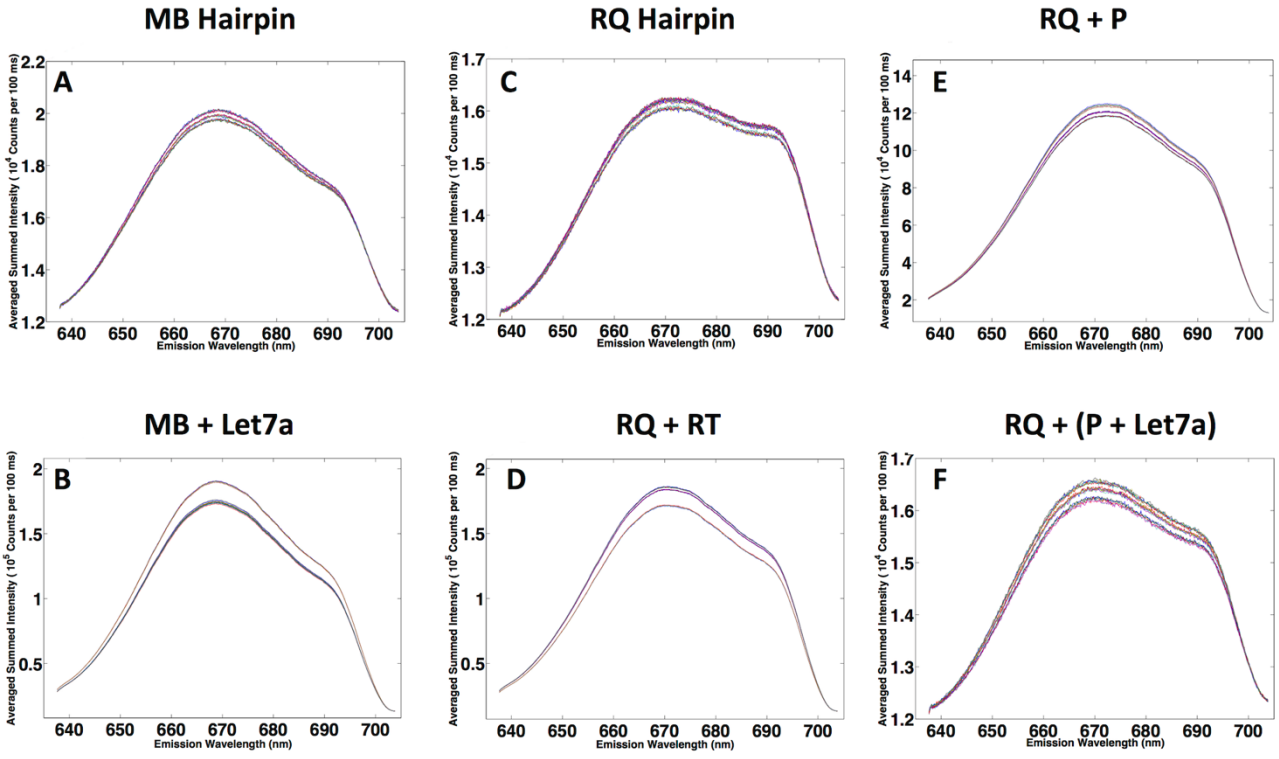

Figure S7. Summary of the three cuvette placements (18 total replicates, 6 replicates per cuvette placement) for various signal-on and signal-off transduction mechanisms (MB, RQ, and (RQ+P)). S4A, S4B and S4C, S4D show full complementarity signal-on for 500 nM MB and RQ, respectively. S4E shows the (RQ+P) complex and S4F shows RQ (hairpin) + (P+let7a). Cuvette placements arise in both the signal-on and signal-off approaches. Using a commercial instrument would greatly mitigate this type of error. Note: The sharp cutoff beginning at 695 nm is due to a 705 nm long-pass dichroic mirror.